SCIENCE CHINA
Chemistry

•ARTICLES•

June 2023 Vol.66 No.6: 1854–1859
https://doi.org/10.1007/s11426-023-1613-x

Electrosynthesis of ^{15}N-labeled amino acids from ^{15}N-nitrite and ketonic acids

Yongmeng Wu[1†], Mengyang Li[1†], Tieliang Li[1], Jinghui Zhao[1], Ziyang Song[1] & Bin Zhang[1,2*]

[1]*Department of Chemistry, School of Science, Institute of Molecular Plus, Tianjin University, Tianjin 300072, China;*
[2]*Tianjin Key Laboratory of Molecular Optoelectronic Science, Key Laboratory of Systems Bioengineering (Ministry of Education), Tianjin University, Tianjin 300072, China*

Received January 20, 2023; accepted May 2, 2023; published online May 10, 2023

^{15}N isotope-labeled amino acids (^{15}N-amino acids) are crucial in the fields of biology, medicine, and chemistry. ^{15}N-amino acids are conventionally synthesized through microbial fermentation and chemical reductive amination of ketonic acids methodologies, which usually require complicated procedures, high temperatures, or toxic cyanide usage, causing energy and environmental concerns. Here, we report a sustainable pathway to synthesize ^{15}N-amino acids from readily available ^{15}N-nitrite ($^{15}NO_2^-$) and biomass-derived ketonic acids under ambient conditions driven by renewable electricity. A mechanistic study demonstrates a ^{15}N-nitrite→$^{15}NH_2OH$→^{15}N-pyruvate oxime→^{15}N-alanine reaction pathway for ^{15}N-alanine synthesis. Moreover, this electrochemical strategy can synthesize six ^{15}N-amino acids with 68%–95% yields. Furthermore, a ^{15}N-labeled drug of ^{15}N-tiopronin, the most commonly used hepatitis treatment drug, is fabricated using ^{15}N-glycine as the building block. Impressively, ^{15}N sources can be recycled by the electrooxidation of $^{15}NH_4^+$ to $^{15}NO_2^-$ with a method economy. This work opens an avenue for the green synthesis of ^{15}N-labeled compounds or drugs.

green synthesis, ^{15}N-labeled amino acids, electrosynthesis, C–N bond, isotope labeling

Citation: Wu Y, Li M, Li T, Zhao J, Song Z, Zhang B. Electrosynthesis of ^{15}N-labeled amino acids from ^{15}N-nitrite and ketonic acids. *Sci China Chem*, 2023, 66: 1854–1859, https://doi.org/10.1007/s11426-023-1613-x

1 Introduction

^{15}N isotope-labeled amino acids (^{15}N-amino acids) provide a safe and effective tracer tool for studying the synthesis of natural products, protein metabolism, and disease diagnosis and treatment in living organisms [1–3]. For instance, Meselson and Stahl [4] used ^{15}N-amino acids to demonstrate the semiretention replication mechanism of DNA in *Escherichia coli*. Moreover, ^{15}N-amino acids can serve as essential building blocks to synthesize ^{15}N-labeled drugs, creating opportunities for lowering the degree of epimerization, reducing the administration dosage, and unveiling the mechanism of action [5,6].

Currently, ^{15}N-amino acids are mainly synthesized through a microbial fermentation method, which usually includes strain breeding, strain culture, and product separation procedures (Figure S1a) [7,8]. Although this method has made continuous advances, it still suffers from low efficiency, high cost for microbial culturing, and complicated procedures for product isolations. In addition, a strain usually produces only one amino acid, making this method poorly universal. Accordingly, thermochemical synthesis *via* ketone acid-reductive ammoniation has been explored for ^{15}N-amino acid synthesis, in which ketonic acids, ^{15}N-ammonia ($^{15}NH_3$), and BH_3CN^- or $HCOO^-$ react to produce ^{15}N-amino acids in organic solvents at elevated temperature (Figure S1b) [9,10]. However, this strategy causes energy and environmental

†These authors contributed equally to this work.
*Corresponding author (email: bzhang@tju.edu.cn)

concerns because it relies on fossil energy, the emission of CO_2, and/or the use of highly toxic cyanide. Therefore, it is highly desirable to develop an alternative strategy to achieve the sustainable and efficient synthesis of ^{15}N-amino acids under ambient conditions.

Electrochemical transformation using renewable electricity as the driving force has emerged as a green and powerful strategy in synthetic chemistry [11–17]. Recently, the electrochemical reduction of nitrite/nitrate (NO_3^-/NO_2^-) has provided a sustainable route for NH_3 production [16,17]. During the reaction, several nitrogen-containing intermediates, such as NO*, NH_2OH*, NH_2*, have been proven. Due to the high activity of these species, the *in-situ* utilization of these nitrogen-containing intermediates offers great potential for constructing organonitrogen compounds *via* the coupling or condensation process with other reaction partners. Electrochemical C–N coupling was revealed by Jiao, Wang *et al.* [18–26] to be a powerful strategy for constructing organonitrogen compounds (*e.g.*, methylamine, amide, urea) by using nitrate or ammonia as the N source. Inspired by these advances, an electrochemical C–N coupling method is supposed to be applied for synthesizing ^{15}N-amino acids. The main challenges of this strategy lie in seeking economical ^{15}N- and C-containing feedstocks and designing a C–^{15}N coupling step of the two precursors to produce ^{15}N-amino acids. Compared to gaseous ^{15}N-ammonia, solid ^{15}N-nitrite is more easily operated, which might be electrochemically reduced to a nucleophilic $^{15}NH_2OH$ intermediate. We speculate that the strong nucleophilic $^{15}NH_2OH$ can attack the electrophilic carbon in ketonic acids to generate ^{15}N-oximes, which can be further electroreduced to ^{15}N-amino acids [27–31]. Additionally, ketonic acids can be derived from lignocellulosic biomass and are a nonfood-competing chemical feedstock. Therefore, the electrochemical synthesis of ^{15}N-amino acids from ^{15}N-nitrite and biomass-derived ketonic acids is of great interest from the perspectives of economy and sustainability.

Herein, we report an electrochemical method to synthesize ^{15}N-amino acids from ^{15}N-nitrite and ketonic acids over a commercial nickel foam (NF) cathode in an aqueous solution under ambient conditions (Figure 1). ^{15}N-alanine with a 93% yield is achieved. Impressively, ^{15}N-ammonium, the major byproduct, can be electrooxidized to ^{15}N-nitrite with a yield of 93%, realizing the recycling property and atomic economy

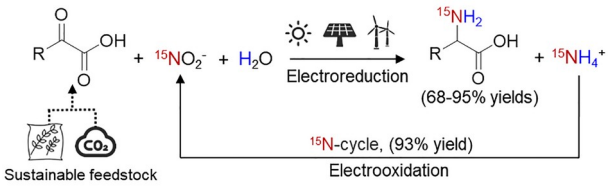

Figure 1 Schematic diagram of the proposed electrosynthesis of ^{15}N-amino acids (color online).

of ^{15}N-nitrite. A ^{15}N-nitrite→$^{15}NH_2OH$→^{15}N-oxime→^{15}N-amino acid pathway is revealed by a series of control experiments, *in-situ* attenuated total reflection Fourier transform infrared (*in-situ* ATR-SEIRAS) spectroscopy, and online differential electrochemical mass spectrometry (DEMS). Furthermore, our method is suitable for synthesizing six ^{15}N-amino acids with 68%–95% yields. A hepatitis treatment drug, ^{15}N-tiopronin is synthesized using ^{15}N-glycine, highlighting the utility of our method.

2 Results and discussion

We begin our study by screening electrodes from a range of commercial metallic materials commonly used in electrocatalytic reactions using pyruvate as the model substrate (unlabeled $NaNO_2$ is used for screening optimal reaction conditions, Figure 2a and Figure S2). After galvanostatic electrolysis for 10 h, the products were identified and quantified by ^{1}H nuclear magnetic resonance (^{1}H NMR), ^{13}C NMR, and liquid chromatography–high resolution mass spectrometry (LC–HRMS). Impressively, alanine is one of the products for most catalysts. Especially, the peaks at 1.2 and 3.5 ppm in the ^{1}H NMR spectrum and 19.3, 59.6, and 175.2 ppm in the ^{13}C NMR spectrum match well with the alanine standard sample (Figure 2b and 2c, Figures S3 and S4). The molecular weight of 90.0553 (*m*/*z*) in the MS spectrum (Figure 2d) is attributed to alanine ($[C_3H_7NO_2+H]^+$). Pyruvate oxime and lactic acid are the main byproducts (Figure S4). Among all eight tested bulk catalysts, Ni foil

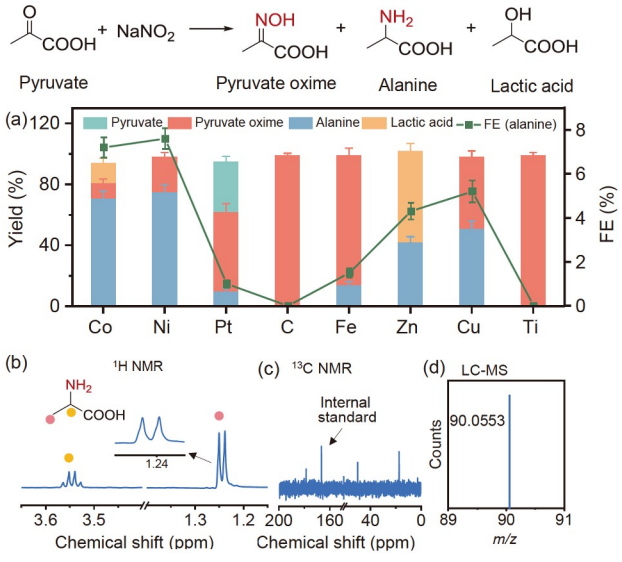

Figure 2 (a) Catalyst screening for alanine electrosynthesis by using pyruvate and $NaNO_2$ as raw materials. Reaction conditions: substrate (0.2 mmol), commercial metal electrodes (working area: 1.4 cm^2), 0.5 mol L^{-1} PBS containing 0.1 mol L^{-1} $NaNO_2$ (20 mL), −30 mA cm^{-2}, 10 h. (b) ^{1}H NMR, (c) ^{13}C NMR, and (d) HRMS tests of the alanine product (color online).

exhibits the highest alanine yield with pyruvate oxime as the only byproduct (Figure 2a). Due to the larger surface area of NF compared with Ni foil, NF was selected as the cathode for the following experiments. Subsequently, the optimal $NaNO_2$ concentration and pH of the electrolyte are screened. pH 2 or pH 5.8 PBS electrolyte containing 0.1 mol L^{-1} $NaNO_2$ is the optimum (Figure S5). Thus, the synthesis of ^{15}N-amino acids is conducted in pH 5.8 PBS with 0.1 mol L^{-1} $Na^{15}NO_2$ as the ^{15}N source.

The linear sweep voltammetry (LSV) curves show an enhanced current density under the coexistence of pyruvic acid and $Na^{15}NO_2$ compared to that of the individual existence of each (Figure 3a). Notably, the LSV curves of $^{15}NO_2^-$ electroreduction exhibits a more negative initial potential and lower current density than that of $^{14}NO_2^-$, indicating the more difficult electroreduction of $^{15}NO_2^-$ (Figure S6). The ^{15}N-alanine yield displays a volcanic shape with increasing applied current density (Figure 3b). A 91% yield and 10% FE of ^{15}N-alanine is obtained at the optimum current density of −39 mA cm^{-2}, and ^{15}N-ammonia is the major byproduct (Figure S7). ^{1}H and ^{13}C NMR spectra of the products produced at the optimum current density are given in Figures 3c and d, Figures S8 and S9, which are similar to those of unlabeled alanine in Figure 2b and Figure S4. Notably, obvious peak splitting is clearly seen from the ^{1}H and ^{13}C NMR spectra, which is not observed in that of unlabeled alanine, demonstrating the acquisition of ^{15}N-labeled alanine. Additionally, the peak at approximately 33 ppm in the ^{15}N-NMR spectrum and the molecular weight of 91.0515 (*m*/*z*) further confirm the successful synthesis of ^{15}N-alanine (Figures 3c, Figure S10). Then, the reaction process is monitored. Pyruvate is consumed completely within 1 h, and the concentration of $Na^{15}NO_2$ decreases rapidly with prolonged reaction time and runs out within 4 h (Figure S11). For the products, ^{15}N-pyruvate oxime is first produced and remains unchanged during the first 4 h. After 4 h, ^{15}N-alanine appears and increases with prolonged reaction time, while ^{15}N-pyruvate oxime shows an opposite variation trend. These

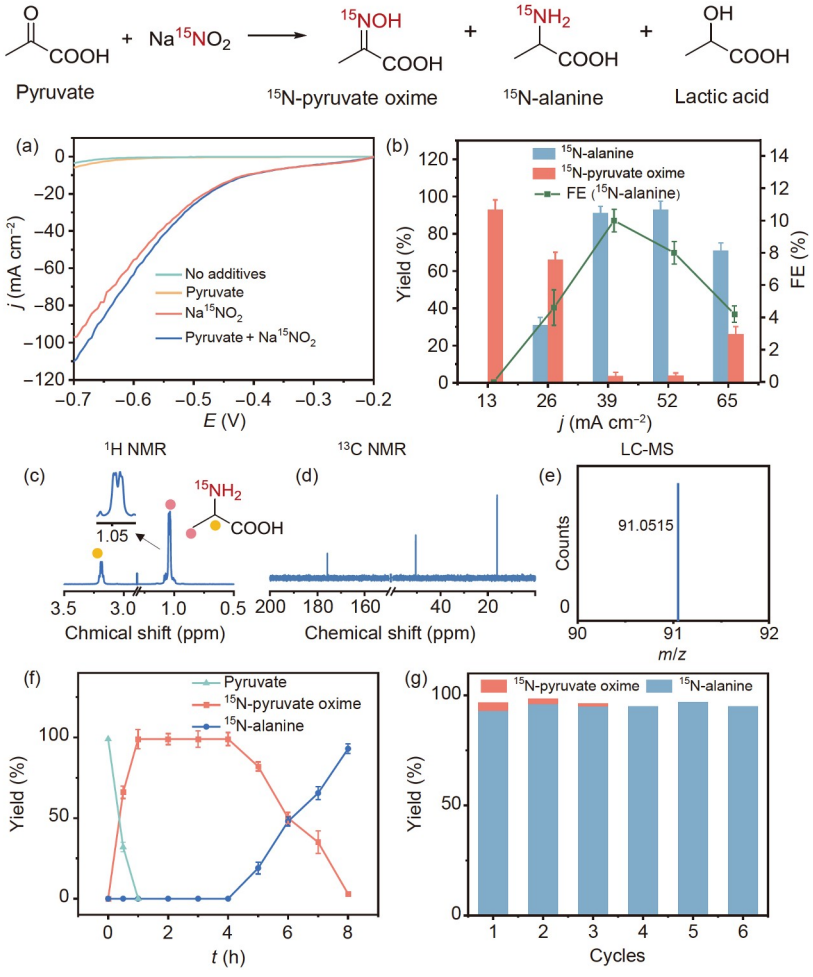

Figure 3 (a) LSV curves of NF in different electrolytes. (b) Potential-dependent yields and FEs of electrolyzed products. Reaction conditions: substrate (0.2 mmol), NF electrode (working area: 1.4 cm^2), 0.5 mol L^{-1} PBS containing 0.1 mol L^{-1} $Na^{15}NO_2$ (20 mL), 8 h. (c) ^{1}H NMR, (d) ^{13}C NMR, and (e) HRMS tests of the ^{15}N-alanine product. (f) Time-dependent yields of electrolyzed products. (g) Durability test for ^{15}N-alanine synthesis at −52 mA cm^{-1} over NF (color online).

results indicate that this reaction is a discontinuous cascade process and the ^{15}N-pyruvate oxime may serve as a key intermediate product for ^{15}N-alanine formation. Subsequently, the durability of the catalyst is assessed, and the performance is maintained well during six cyclic tests. No ^{15}N-alanine is detected when removing electricity, $Na^{15}NO_2$, and pyruvic acid, demonstrating the electrically driven process with $Na^{15}NO_2$ and pyruvic acid as the ^{15}N and C sources, respectively (Entries 1–3 in Table 1 and Figure S12). Note that the major byproduct of $^{15}NH_4^+$ can be electrooxidized to $^{15}NO_2^-$ with a yield of 93% (Figure S13), thus realizing the recycling of the ^{15}N source with the methodology economy.

The reaction pathway is elucidated by performing a series of control experiments, *in-situ* ATR-SEIRAS, and online DEMS tests. Commonly, ^{15}N-pyruvate oxime, lactic acid, and ^{15}N-alanine are the main possible products under electrochemical conditions. The side product of lactic acid is formed by the hydrogenation of pyruvate, which can be efficiently inhibited by increasing the concentration of $Na^{15}NO_2$ (Figure S5a). Because the yields of ^{15}N-pyruvate oxime and ^{15}N-alanine exhibit an opposite trend as the reaction proceeds (Figure 3f), we speculate that ^{15}N-pyruvate oxime serves as an intermediate, which is first generated and further hydrogenated to ^{15}N-alanine. This hypothesis is further verified by using pyruvate oxime as the initial reactant (Entry 4 in Table 1 and Figure S14). As expected, alanine is detected as the only product after the electroreduction of pyruvate oxime in pH 5.8 PBS for 5 h, further verifying that the reaction proceeded through a cascade process involving a ^{15}N-pyruvate oxime intermediate.

The mechanism of the formation of ^{15}N-pyruvate oxime was further studied. ^{15}NO* (1,581 cm^{-1}), $^{15}NH_2$* (1,466 cm^{-1}) and $^{15}NH_2OH$* (1,181 cm^{-1}) are detected by *in-situ* ATR-SEIRAS and online DEMS (Figure 4a–4c) [32]. These wavenumbers are lower than those of unlabeled NO* (1,590 cm^{-1}), NH_2* (1,488 cm^{-1}), and NH_2OH* (1,192 cm^{-1})

Table 1 List of control experiments

Entry	N-source	C-source	j (mA cm^{-2}) (duration)	Electrolytes	Product
1	/	Pyruvate	−52 (8 h)	0.5 mol L^{-1} PBS+0.2 mmol pyruvate	No product
2	$^{15}NO_2^-$	/	−52 (8 h)	0.5 mol L^{-1} PBS+0.1 mol L^{-1} $Na^{15}NO_2$	No product
3	$^{15}NO_2^-$	Pyruvate	No bias (8 h)	0.5 mol L^{-1} PBS+0.1 mol L^{-1} $Na^{15}NO_2$+0.2 mmol pyruvate	No product
4	/	Pyruvate oxime	−52 (8 h)	0.5 mol L^{-1} PBS+0.2 mmol pyruvate oxime	Alanine
5	$^{15}NH_4^+$	Pyruvate	−52 (8 h)	0.5 mol L^{-1} PBS+0.1 mol L^{-1} $^{15}NH_4Cl$+0.2 mmol pyruvate	No product
6	$^{15}NH_2OH$	Pyruvate	−52 (8 h)	0.5 mol L^{-1} PBS+0.2 mmol $^{15}NH_2OH$+0.2 mmol pyruvate	^{15}N-Alanine
7	NO	Pyruvate	−52 (8 h)	0.5 mol L^{-1} PBS+0.2 mmol pyruvate	Alanine
8	$^{15}NH_2OH$	Pyruvate	No bias (5 min)	0.5 mol L^{-1} PBS+0.2 mmol $^{15}NH_2OH$+0.2 mmol pyruvate	^{15}N-pyruvate oxime

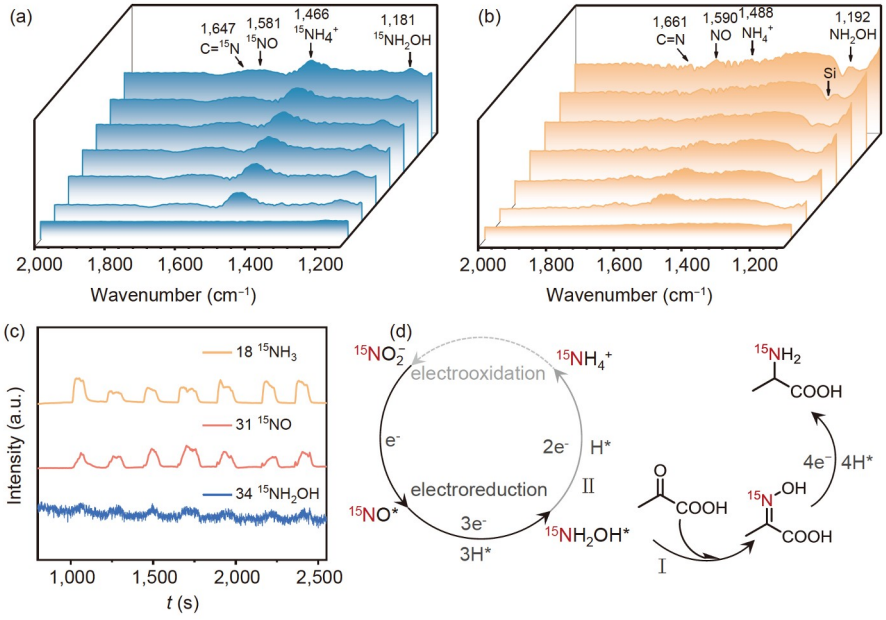

Figure 4 Time-dependent *in-situ* ATR-SEIRAS using pyruvate as the C-source and (a) $^{15}NO_2^-$ and (b) $^{14}NO_2^-$ as the N-source. (c) Online DEMS results of ^{15}N-nitrite electroreduction in 0.5 mol L^{-1} PBS at −0.7 V *vs.* Ag/AgCl. (d) The proposed reaction pathway for the electrosynthesis of ^{15}N-alanine from pyruvate and $^{15}NO_2^-$ (color online).

with $NaNO_2$ as the N source. These redshifts are ascribed to the isotope effect [33]. Moreover, a new peak of C=^{15}N (1,647 cm^{-1}) indexed to the –C=^{15}N–OH group appears and is enhanced with increasing electrolysis time, further demonstrating the formation of the ^{15}N-pyruvate oxime. Online DEMS further confirms that ^{15}NO* (31), $^{15}NH_3$ (18), and $^{15}NH_2OH$* (34) formed during the reaction. Therefore, to verify the ^{15}N-containing active species for oxime formation, control experiments using pyruvic acid as the C source and ^{15}NO, $^{15}NH_2OH$, and $^{15}NH_4^+$ as the ^{15}N sources were carried out. Neither ^{15}N-pyruvate oxime nor ^{15}N-alanine products were detected when using $^{15}NH_4^+$ as the ^{15}N source, excluding the involvement of $^{15}NH_3$ in ^{15}N-pyruvate oxime formation (Entry 5 in Table 1 and Figure S15). Instead, when using ^{15}NO or $^{15}NH_2OH$ as the ^{15}N sources, ^{15}N-pyruvate oxime and ^{15}N-alanine products are formed (Entries 6 and 7 in Table 1 and Figure S15). Considering that $^{15}NH_2OH$ is the more reduced intermediate than ^{15}NO in $^{15}NO_2^-$ RR, it is reasonable to regard $^{15}NH_2OH$ as the ^{15}N source to form ^{15}N-pyruvate oxime. ^{15}N-pyruvate oxime can be produced as soon as $^{15}NH_2OH$ and pyruvic acid are mixed at room temperature even without electricity, suggesting a spontaneous process for the formation of oxime (Entry 8 in Table 1 and Figure S16). The fast C–N coupling kinetics due to the strong nucleophilic property of hydroxyamine inhibits the deep reduction of $^{15}NH_2OH$, thus leading to the effective formation of pyruvate oxime [19,27–29]. Based on the above discussion, the mechanism is proposed in Figure 4d. The electroreduction of $^{15}NO_2^-$ first proceeds following the sequence of $^{15}NO_2^- \rightarrow {}^{15}NO^* \rightarrow {}^{15}NH_2OH^*$ on the catalyst surface. Then, the adsorbed pyruvic acid is rapidly attacked by nucleophilic $^{15}NH_2OH$ to generate ^{15}N-pyruvate oxime by losing a molecule of H_2O, which is further electroreduced to ^{15}N-alanine (**Path I**). Because the concentration of $^{15}NO_2^-$ is much higher than that of pyruvate, the amount of $^{15}NH_2OH$ produced on the catalyst surface is greater than that of pyruvate. Thus, the unreacted $^{15}NH_2OH$ is further reduced to $^{15}NH_4^+$, which can be recycled by the electrooxidation to $^{15}NO_2^-$ for next wave utilization (**Path II**).

To show the universality of our approach, we apply our method to the electrosynthesis of other ^{15}N-amino acids. Delightfully, this method is suitable for synthesizing different types of ^{15}N-amino acids (**2a**–**2f**) with good yields (68%–95%) (Figures 5a, and Figures S17–S21), and some of them are commonly used drug-building blocks [34]. For example, by employing ^{15}N-glycine as the building block, ^{15}N-tiopronin (30% overall isolated yield), the most efficient drug to treat hepatitis, was successfully synthesized (Figure 5b and Figure S22) [35]. It is reasonable to speculate that the incorporation of ^{15}N in tiopronin can slow down the metabolic process due to the more stable C–^{15}N bond than the C–N bond [5], thus increasing the effective drug duration *in vivo* and lowering the dose. These results show the application potential of our method in ^{15}N-labeled drug synthesis and metabolism.

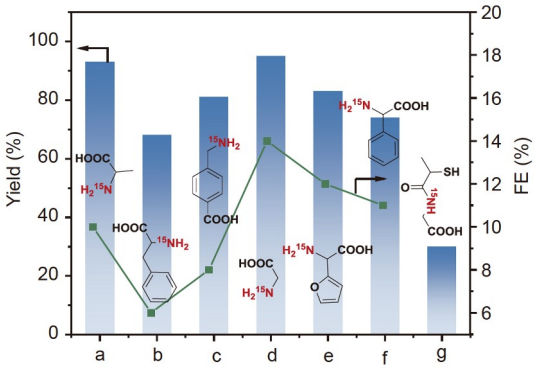

Figure 5 Electrosynthesis of ^{15}N-amino acids (a–f, NMR yields are reported) and ^{15}N-tiopronin (g, an isolated yield is reported) (color online).

3 Conclusions

In conclusion, we demonstrate an electrochemical strategy to synthesize ^{15}N-amino acids through the co-reduction of $Na^{15}NO_2$ and ketonic acids under ambient conditions over the NF cathode. Mechanistic studies reveal that the electrochemical reaction undergoes multistep processes of $^{15}NO_2^-$ RR to $^{15}NH_2OH$, the condensation of $^{15}NH_2OH$ and pyruvate to ^{15}N-pyruvate oxime, and the subsequent hydrogenation of ^{15}N-pyruvate oxime to ^{15}N-alanine. Moreover, this electrochemical strategy can be used to synthesize other ^{15}N-amino acids with 68%–95% yields, demonstrating the good universality of our method. Furthermore, a ^{15}N-labeled hepatitis treatment drug of ^{15}N-tiopronin is synthesized using ^{15}N-glycine as the building block, which may provide an opportunity to study disease treatment and drug metabolism. Our study not only offers a strategy for the room-temperature and green synthesis of ^{15}N-amino acids but also opens a sustainable avenue to construct ^{15}N-labeled compounds.

Acknowledgements This work is supported by the National Natural Science Foundation of China (22271213) and the National Postdoctoral Science Foundation of China (2022M722357).

Conflict of interest The authors declare no conflict of interest.

Supporting information The supporting information is available online at chem.scichina.com and link.springer.com/journal/11426. The supporting materials are published as submitted, without typesetting or editing. The responsibility for scientific accuracy and content remains entirely with the authors.

1 Velyvis A, Vaynberg J, Yang Y, Vinogradova O, Zhang Y, Wu C, Qin J. *Nat Struct Mol Biol*, 2003, 10: 558–564
2 Shuker SB, Hajduk PJ, Meadows RP, Fesik SW. *Science*, 1996, 274: 1531–1534
3 Ramirez B, Durst MA, Lavie A, Caffrey M. *Sci Rep*, 2019, 9: 12798

4 Meselson M, Stahl FW. *Proc Natl Acad Sci USA*, 1958, 44: 671–682
5 Wang H, Dong Y, Zheng C, Sandoval CA, Wang X, Makha M, Li Y. *Chem*, 2018, 4: 2883–2893
6 Liu C, Chen Z, Yan H, Xi S, Yam KM, Gao J, Du Y, Li J, Zhao X, Xie K, Xu H, Li X, Leng K, Pennycook SJ, Liu B, Zhang C, Koh MJ, Loh KP. *Sci Adv*, 2019, 5: eaay1537
7 D'Este M, Alvarado-Morales M, Angelidaki I. *Biotechnol Adv*, 2018, 36: 14–25
8 Whittaker JW. *Methods Mol Biol*, 2007, 389: 175–188
9 Borch RF, Bernstein MD, Durst HD. *J Am Chem Soc*, 1971, 93: 2897–2904
10 Ogo S, Uehara K, Abura T, Fukuzumi S. *J Am Chem Soc*, 2004, 126: 3020–3021
11 Wu Y, Liu C, Wang C, Lu S, Zhang B. *Angew Chem Int Ed*, 2020, 59: 21170–21175
12 Liu X, Liu R, Qiu J, Cheng X, Li G. *Angew Chem Int Ed*, 2020, 59: 13962–13967
13 Liu S, Cheng X. *Nat Commun*, 2022, 13: 425
14 Ko BH, Hasa B, Shin H, Zhao Y, Jiao F. *J Am Chem Soc*, 2022, 144: 1258–1266
15 Panja S, Ahsan S, Pal T, Kolb S, Ali W, Sharma S, Das C, Grover J, Dutta A, Werz DB, Paul A, Maiti D. *Chem Sci*, 2022, 13: 9432–9439
16 Wang Y, Yu Y, Jia R, Zhang C, Zhang B. *Natl Sci Rev*, 2019, 6: 730–738
17 Han S, Li H, Li T, Chen F, Yang R, Yu Y, Zhang B. *Nat Catal*, 2023, DOI:10.1038/s41929-023-00951-2
18 Jouny M, Lv JJ, Cheng T, Ko BH, Zhu JJ, Goddard III WA, Jiao F. *Nat Chem*, 2019, 11: 846–851
19 Wu Y, Jiang Z, Lin Z, Liang Y, Wang H. *Nat Sustain*, 2021, 4: 725–730
20 Tao Z, Rooney CL, Liang Y, Wang H. *J Am Chem Soc*, 2021, 143: 19630–19642
21 Rooney CL, Wu Y, Tao Z, Wang H. *J Am Chem Soc*, 2021, 143: 19983–19991
22 Li J, Zhang Y, Kuruvinashetti K, Kornienko N. *Nat Rev Chem*, 2022, 6: 303–319
23 Li J, Kornienko N. *Chem Sci*, 2022, 13: 3957–3964
24 Guo C, Zhou W, Lan X, Wang Y, Li T, Han S, Yu Y, Zhang B. *J Am Chem Soc*, 2022, 144: 16006–16011
25 Meng N, Ma X, Wang C, Wang Y, Yang R, Shao J, Huang Y, Xu Y, Zhang B, Yu Y. *ACS Nano*, 2022, 16: 9095–9104
26 Huang Y, Wang Y, Wu Y, Yu Y, Zhang B. *Sci China Chem*, 2021, 65: 204–206
27 Fukushima T, Yamauchi M. *Chem Commun*, 2019, 55: 14721–14724
28 Kim JE, Jang JH, Lee KM, Balamurugan M, Jo YI, Lee MY, Choi S, Im SW, Nam KT. *Angew Chem Int Ed*, 2021, 60: 21943–21951
29 Kulisch J, Nieger M, Stecker F, Fischer A, Waldvogel SR. *Angew Chem Int Ed*, 2011, 50: 5564–5567
30 Edinger C, Kulisch J, Waldvogel SR. *Beilstein J Org Chem*, 2015, 11: 294–301
31 Lips S, Waldvogel SR. *ChemElectroChem*, 2019, 6: 1649–1660
32 Pérez-Gallent E, Figueiredo MC, Katsounaros I, Koper MTM. *Electrochim Acta*, 2017, 227: 77–84
33 Zhu S, Jiang B, Cai WB, Shao M. *J Am Chem Soc*, 2017, 139: 15664–15667
34 Pirali T, Serafini M, Cargnin S, Genazzani AA. *J Med Chem*, 2019, 62: 5276–5297
35 Li J, Qiu X, Guo W, Yan B, Zhang S. *Med Oncol*, 2015, 32: 238